

# Comparison of Particle Light Scattering and Fine Particulate Matter Mass in Central California

Judith C. Chow, John G. Watson, Kihong Park, Douglas H. Lowenthal, Norman F. Robinson  
*Desert Research Institute, Reno, NV*

Kihong Park  
*Gwangju Institute of Science and Technology, Gwangju, Korea*

Karen A. Magliano  
*California Air Resources Board, Sacramento, CA*

## ABSTRACT

Particle light scattering ( $B_{sp}$ ) from nephelometers and fine particulate matter ( $PM_{2.5}$ ) mass determined by filter samplers are compared for summer and winter at 35 locations in and around California's San Joaquin Valley from December 2, 1999 to February 3, 2001. The relationship is described using particle mass scattering efficiency ( $\sigma_{sp}$ ) derived from linear regression of  $B_{sp}$  on  $PM_{2.5}$  that can be applied to estimated  $PM_{2.5}$  from nephelometer data within the 24-hr filter sampling periods and between the every-6th-day sampling frequency. An average of  $\sigma_{sp} = 4.9 \text{ m}^2/\text{g}$  was found for all of the sites and seasons; however,  $\sigma_{sp}$  averaged by site type and season provided better  $PM_{2.5}$  estimates. On average, the  $\sigma_{sp}$  was lower in summer than winter, consistent with lower relative humidities, lower fractions of hygroscopic ammonium nitrate, and higher contributions from fugitive dust. Winter average  $\sigma_{sp}$  were similar at non-source-dominated sites, ranging from  $4.8 \text{ m}^2/\text{g}$  to  $5.9 \text{ m}^2/\text{g}$ . The  $\sigma_{sp}$  was  $2.3 \text{ m}^2/\text{g}$  at the roadside,  $3.7 \text{ m}^2/\text{g}$  at a dairy farm, and  $4.1 \text{ m}^2/\text{g}$  in the Kern County oilfields. Comparison of  $B_{sp}$  from nephelometers with and without a  $PM_{2.5}$  inlet at the Fresno Super-site showed that coarse particles contributed minor amounts to light scattering. This was confirmed by poorer correlations between  $B_{sp}$  and coarse particulate matter measured during a fall sampling period.

## INTRODUCTION

Nephelometers<sup>1-3</sup> quantify the light scattered by particles by drawing them into an enclosed chamber, shining a bright light through the particle cloud, and measuring the amount of light scattered from its original direction. This

### IMPLICATIONS

Relatively inexpensive and portable nephelometers and  $PM_{2.5}$  samplers can be used to deploy a large spatial air-monitoring network. Relationships between  $B_{sp}$  and  $PM_{2.5}$  can be reliably established, but these differ by site type and sampling period. Nephelometers should not be used in the absence of some collocated  $PM_{2.5}$  filter sampling at the same or similar measurement sites.

particle light scattering ( $B_{sp}$ , in units of inverse megameters [ $\text{Mm}^{-1}$ ]) is often correlated with mass concentrations of suspended particulate matter (PM, in units of  $\mu\text{g}/\text{m}^3$ ). Using the relationship  $B_{sp} = \sigma_{sp} \times \text{PM}$ , where  $\sigma_{sp}$  is the particle mass scattering efficiency ( $\text{m}^2/\text{g}$ ), several researchers have derived empirical relationships between  $B_{sp}$  and PM that enable one to be estimated by measuring the other.<sup>4-12</sup> The value of  $\sigma_{sp}$  varies with particle size distribution, particle composition, and relative humidity (RH),<sup>13</sup> so it must be derived for different seasons, monitoring locations, and even for different samples. In addition,  $\sigma_{sp}$  is most consistent and physically meaningful when it is applied to the fine particulate matter ( $PM_{2.5}$ ) size fraction under dry conditions. Most  $PM_{2.5}$  particles have diameters comparable to the wavelength ( $\lambda$ ) of the incident light, resulting in high  $\sigma_{sp}$ . Particles larger than  $2.5 \mu\text{m}$  tend to scatter light less uniformly than smaller particles, and for most nephelometers a portion of the forward-scattered signal is truncated.<sup>14-21</sup> For these reasons, nephelometer  $B_{sp}$  is most accurately used as a surrogate for  $PM_{2.5}$  mass concentrations, rather than for larger size fractions.

Nephelometers were deployed along with 24-hr  $PM_{2.5}$  filter samplers during the California Regional  $PM_{10}/PM_{2.5}$  Air Quality Study (CRPAQS)<sup>22</sup> to (1) determine  $\sigma_{sp}$  and its variability with location and season; (2) understand how  $PM_{2.5}$  changes during the 24-hr filter sampling period; (3) evaluate  $PM_{2.5}$  levels on days between the every-6th-day filter sampling frequency at most sites; and (4) estimate  $PM_{2.5}$  levels at sites that did not have collocated  $PM_{2.5}$  filter measurements. The combination of inexpensive nephelometers<sup>23-25</sup> and filter samplers<sup>26</sup> that can be located on rooftops and power poles provides the possibility of obtaining large amounts of spatial and temporal information at minimal cost. The methods illustrated here can be applied in a wide variety of locations.

In this study, relationships between  $B_{sp}$  and  $PM_{2.5}$  mass are derived for 35 monitoring sites in central California. A predictability function is developed that can be used to estimate  $PM_{2.5}$  mass from  $B_{sp}$ . Differences caused by site type, sampling location, sampling period, and ambient  $PM_{2.5}$  levels are examined to determine when and where  $B_{sp}$  can be used as a surrogate for  $PM_{2.5}$  mass.

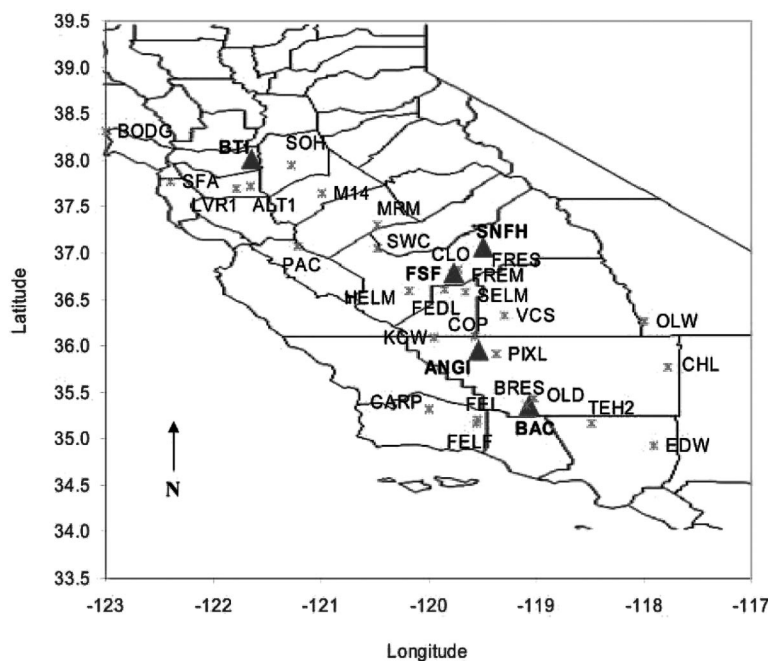


**Figure 1.** CRPAQS monitoring sites (5 anchor sites [▲] and 30 satellite sites [\*]) with collocated Radiance Research M903 nephelometer and  $PM_{2.5}$  filter samplers (Map not to scale).

Fine particle light scattering ( $B_{sp}$ ) measured with  $PM_{2.5}$  size-selective inlets is compared with total  $B_{sp}$  to evaluate the contribution from coarse particle scattering. Different nephelometers and filter sampling methods for  $B_{sp}$  and  $PM_{2.5}$  mass are also compared.

## METHODS

At the CRPAQS sites shown in Figure 1, Radiance Research (Seattle, WA) M903 nephelometers ( $\lambda = 530$  nm) were collocated with Desert Research Institute (DRI; Reno, NV)  $PM_{2.5}$  sequential filter samplers (SFS) at five anchor sites (Bethel Island [BTI], Sierra Nevada Foothills [SNFH], Fresno Supersite<sup>27</sup> [FSF], Angiola [ANGI], and Bakersfield [BAC]). These were also collocated with Airmetrics (Eugene, OR) battery-powered  $PM_{2.5}$  MiniVol filter samplers at 30 satellite sites (Table 1). Most sites were located within California's San Joaquin Valley (SJV) except for the Bodega Bay (BODG), San Francisco (SFA), Olancho (OLW), China Lake (CHL), Tehachapi Pass (TEH2), and Edwards (EDW) sites. Table 1 summarizes locations (longitude, latitude), elevations, filter sampler types, site classifications and characterizations, and sampling periods.

Air was drawn into the nephelometer through an annular inlet (capped inlet tube with a 0.5-cm annulus) with a smart heater. The smart heater consists of a tube wrapped with heating tape that only applies heat when the RH at the outlet exceeds 72%. This heating reduces the enhancement of  $B_{sp}$  caused by water uptake of hygroscopic particles under high RH, while minimizing the evaporation of volatile material such as secondary ammonium nitrate ( $NH_4NO_3$ ).<sup>23,24</sup>

The 24-hr (midnight-to-midnight) filter samples were collected every 6th day over a 14-month period (December 2, 1999, to February 3, 2001). The 24-hr SFS samples were taken at the FSF, ANGI, and BAC sites, starting on

December 2, 1999, and at the BTI and SNFH sites, starting on December 2, 2000. Winter intensive operating periods (December 15, 2000 to February 3, 2001) included 5-times-per-day sampling for 15 days at the five anchor sites and 24-hr samples for 13 days at 25 satellite sites. The  $B_{sp}$  data were averaged over the 24-hr sampling periods for comparison.

At FSF, Radiance nephelometers with and without a  $PM_{2.5}$  size-selective inlet were collocated to determine the extent to which coarse particles affect  $B_{sp}$ . An Optec NGN-2 ambient temperature low-truncation nephelometer (Lowell, MI,  $\lambda = 550$  nm) measured total  $B_{sp}$ , including the portion caused by hygroscopicity and coarse particles. Non-integrating nephelometers included the TSI Dust-Trak (DT8520; Shoreview, MN,  $\lambda = 780$  nm) and the GreenTek photometer (GT640A; Atlanta, GA,  $\lambda = 780$  nm). These measure forward scattering at longer wavelengths and are more sensitive to coarse particles than integrating nephelometers that measure side-scatter at shorter wavelengths. Although the DustTrak and GreenTek units measure light scattering, they internally apply a  $\sigma_{sp}$  and give mass per unit volume outputs. Hourly average  $PM_{2.5}$  and  $PM_{10}$  were measured at FSF with Met One (Grants Pass, OR) beta attenuation monitors (BAMs) without water vapor denuders and Rupprecht & Patashnick (Albany, NY) tapered element oscillating microbalances (TEOMs) operated at 50 °C. Also at FSF,  $PM_{2.5}$  filter samples were taken with SFS, MiniVol, and Federal Reference Method (FRM; RAAS 100; Anderson Instruments, Smyrna, GA) samplers.

Nonweighted least-squares regression of  $B_{sp}$  on  $PM_{2.5}$  mass was used to estimate  $\sigma_{sp}$  as the regression slope. A multiple linear regression was conducted when  $B_{sp}$ ,  $PM_{2.5}$ , and  $PM_{10-2.5}$  ( $PM_{10} - PM_{2.5}$ ) mass were available.

**Table 1.** Central California sampling sites with collocated  $B_{sp}$  and  $PM_{2.5}$  mass measurements.

Site Code	Site	Longitude	Latitude	Elevation (m)	$PM_{2.5}$ Filter Sampler	Site Characteristics	Sampling Period (data available)
ACP	Angels Camp	-120.491	38.006	373	MiniVol <sup>a</sup>	Intrabasin gradient	Nov. 30, 2000 to Jan. 31, 2001
ALT1	Altamont Pass	-121.660	37.718	350	MiniVol	Interbasin transport	Jan. 28, 2000 to Jan. 31, 2001
ANGI <sup>c</sup>	Angiola Trailer—ground level Bakersfield—5558 California Street	-119.538	35.948	60	SFS <sup>b</sup>	Intrabasin gradient, vertical gradient, visibility	Feb. 1, 2000 to Feb. 3, 2001
BAC <sup>c</sup>	Street	-119.063	35.357	119	SFS	Community exposure, visibility	Jan. 6, 2000 to Feb. 3, 2001
BODG	Bodega Bay Residential area near BAC	-123.073	38.319	17	MiniVol	Boundary/background	Dec. 23, 1999 to Jan. 31, 2001
BRES	with woodburning	-119.084	35.358	117	MiniVol	Source—woodburning	Nov. 29, 2000 to Jan. 31, 2001
BTI <sup>c</sup>	Bethel Island	-121.642	38.006	2	SFS	Interbasin transport	Dec. 1, 2000 to Feb. 3, 2001
CARP	Carrizo Plain	-119.996	35.314	598	MiniVol	Intrabasin gradient, visibility Visibility, desert environment	Jul. 1, 2000 to Jan. 31, 2001
CHL	China Lake	-117.776	35.774	684	MiniVol	outside of SJV	Feb. 17, 2000 to Jan. 31, 2001
CLO	Clovis-908 N Villa Avenue	-119.716	36.819	108	MiniVol	Community exposure	Dec. 12, 2000 to Jan. 31, 2001
COP	Corcoran-Patterson Avenue	-119.566	36.102	63	MiniVol	Community exposure	Oct. 9, 2000 to Jan. 31, 2001
EDI	Edison	-118.957	35.350	118	MiniVol	Intrabasin gradient Intrabasin gradient, visibility, Desert environment outside of SJV	Dec. 5, 2000 to Jan. 31, 2001
EDW	Edwards Air Force Base	-117.904	34.929	724	MiniVol	SJV	Feb. 10, 2000 to Jan. 31, 2001
FEDL	Feedlot or Dairy	-119.855	36.611	76	MiniVol	Source—dairy	Jul. 7, 2000 to Jan. 31, 2001
FEL	Fellows	-119.546	35.203	359	MiniVol	Source—oilfields Source—oilfields Intrabasin gradient	Feb. 1, 2000 to Jan. 31, 2001
FELF	Foothills above Fellows	-119.557	35.171	512	MiniVol	gradient	Mar. 18, 2000 to Jan. 31, 2001
FREM	Fresno-motor vehicle Residential area near FSF	-119.783	36.780	96	MiniVol	Source—motor vehicle	Jan. 10, 2000 to Jan. 29, 2001
FRES	with woodburning	-119.768	36.783	97	MiniVol	Source—woodburning	Jan. 30, 2000 to Jan. 31, 2001
FSF <sup>c</sup>	Fresno-3425 First Street	-119.773	36.782	97	SFS	Community exposure, visibility	Jan. 21, 2000 to Feb. 3, 2001
HELM	Helm-Central Fresno County	-120.177	36.591	55	MiniVol	Intrabasin gradient	Nov. 30, 2000 to Jan. 31, 2001
KCW	Kettleman City	-119.948	36.095	69	MiniVol	Intrabasin gradient	Nov. 27, 2000 to Jan. 31, 2001
LVR1	Livermore-793 Rincon at Pine	-121.784	37.688	138	MiniVol	Interbasin transport	Nov. 19, 2000 to Jan. 31, 2001
M14	Modesto 14th Street	-120.994	37.642	28	MiniVol	Community exposure	Nov. 11, 2000 to Jan. 31, 2001
MRM	Merced-Midtown	-120.481	37.308	53	MiniVol	Community exposure	Dec. 1, 2000 to Jan. 31, 2001
OLD	Oildale-Manor	-119.017	35.438	180	MiniVol	Community exposure Background, desert environment	Nov. 28, 2000 to Jan. 31, 2001
OLW	Olancho-Walker Creek Rd	-117.993	36.268	1124	MiniVol	outside of SJV	Feb. 17, 2000 to Jan. 31, 2001
PAC	Pacheco Pass	-121.222	37.073	452	MiniVol	Interbasin transport	Feb. 3, 2000 to Jan. 31, 2001
PIXL	Pixley Wildlife Refuge	-119.376	35.914	69	MiniVol	Interbasin gradient, rural	Jan. 26, 2000 to Jan. 31, 2001
SELM	Selma Airport	-119.660	36.583	94	MiniVol	Community exposure	Mar. 16, 2000 to Jan. 31, 2001
SFA	San Francisco-10 Arkansas	-122.399	37.766	6	MiniVol	Community exposure Intrabasin gradient, vertical gradient, visibility	Nov. 19, 2000 to Jan. 31, 2001
SNFH <sup>c</sup>	Sierra Nevada Foothills	-119.496	37.063	589	SFS	gradient, visibility	Dec. 1, 2000 to Feb. 3, 2001
SOH	Stockton-Hazelton Street	-121.269	37.950	8	MiniVol	Community exposure	Nov. 29, 2000 to Jan. 31, 2001
SWC	SW Chowchilla	-120.472	37.048	43	MiniVol	Intrabasin gradient	Nov. 29, 2000 to Jan. 31, 2001
TEH2	Tehachapi Pass	-118.482	35.168	1229	MiniVol	Interbasin transport, visibility	Feb. 10, 2000 to Jan. 31, 2001
VCS	Visalia-North Church Street	-119.291	36.333	102	MiniVol	Community exposure	Nov. 30, 2000 to Jan. 31, 2001

<sup>a</sup>Battery-powered MiniVol samplers (Airmetrics, Eugene, OR) equipped with  $PM_{10}$  and  $PM_{2.5}$  inlets (in series) or  $PM_{10}$  inlets operated at a 5 L/min flow rate; MiniVol samplers are shown to acquire  $PM_{2.5}$  mass equivalent to  $PM_{2.5}$  FRM compliance sampler; <sup>b</sup>Desert Research Institute (Reno, NV) SFS equipped with Bendix 240 cyclone  $PM_{2.5}$  inlets and anodized aluminum nitric acid denuders operated at 113 L/min with 20 L/min flow rate through each sampling port; <sup>c</sup>Anchor sites; others are satellite sites.

## RESULTS AND DISCUSSION

### Spatial Variability of Light Scattering, $PM_{2.5}$ Mass, and Scattering Efficiencies

Comparisons of daily average  $B_{sp}$  and  $PM_{2.5}$  mass grouped by site characteristics and season (winter and summer) are summarized in Table 2. As shown in Figure 2a, the 24-hr winter average  $B_{sp}$  varied by a factor of 21, from  $14 \text{ Mm}^{-1}$  at the OLW site to  $299\text{--}303 \text{ Mm}^{-1}$  at the Bakersfield residential (BRES), Edison (EDI), and Visalia (VCS) sites. The 24-hr winter average  $PM_{2.5}$  mass varied by a factor of

46, from  $1.3 \mu\text{g}/\text{m}^3$  at the CHL site to  $60.5 \mu\text{g}/\text{m}^3$  at the Fresno roadside (FREM) site. Winter average  $PM_{2.5}$  concentrations at urban sites (e.g., BRES,  $53.9 \mu\text{g}/\text{m}^3$ ; FRES,  $57.4 \mu\text{g}/\text{m}^3$ ; FREM,  $60.5 \mu\text{g}/\text{m}^3$ ) were twice the wintertime all-site average ( $28.9 \mu\text{g}/\text{m}^3$ ). The lowest  $B_{sp}$  and  $PM_{2.5}$  averages occurred at OLW ( $14 \text{ Mm}^{-1}$ ,  $3.3 \mu\text{g}/\text{m}^3$ ), CHL ( $15 \text{ Mm}^{-1}$ ,  $1.3 \mu\text{g}/\text{m}^3$ ), and EDW ( $26 \text{ Mm}^{-1}$ ,  $5.4 \mu\text{g}/\text{m}^3$ ); these were desert sites outside of the SJV.

The spatial variability of  $\sigma_{sp}$  for the winter sampling period is shown in Figure 3. The desert sites, OLW, CHL,

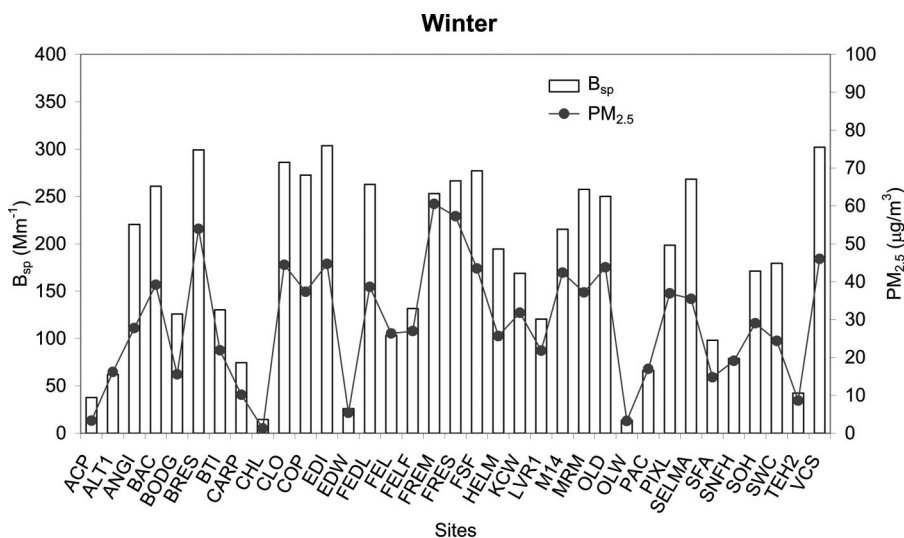
**Table 2.** Comparisons of  $\sigma_{sp}$  derived from  $B_{sp}$  determined by a Radiance nephelometer and  $PM_{2.5}$  mass determined by SFS (anchor sites) and MiniVol sampler (satellite sites).

Site Code	Site Characteristics	Observables		Measurement Method		Corr. <sup>b</sup> (r)	N <sup>a</sup>	Slope <sup>b</sup> ± Standard Error (m <sup>2</sup> /g)	Intercept <sup>b</sup> ± Standard Error (Mm <sup>-1</sup> )	Winter Slope (m <sup>2</sup> /g)	Winter Intercept (Mm <sup>-1</sup> )	Summer Slope (m <sup>2</sup> /g)	Summer Intercept (Mm <sup>-1</sup> )
		y	x	y	x								
BAC <sup>c</sup>	Community exposure	$B_{sp}$	$PM_{2.5}$	Nephelometer	SFS	0.91	366	$6.1 \pm 0.2$	$-28.7 \pm 66.9$	6.34	-1.11	1.40	13.89
CLO	Community exposure	$B_{sp}$	$PM_{2.5}$	Nephelometer	MiniVol	0.85	10	$5.2 \pm 1.2$	$64.4 \pm 76.7$	5.16	64.43	NA <sup>b</sup>	NA
COP	Community exposure	$B_{sp}$	$PM_{2.5}$	Nephelometer	MiniVol	0.89	18	$4.5 \pm 0.6$	$71.7 \pm 26.3$	4.03	107.31	NA	NA
FSF <sup>c</sup>	Community exposure	$B_{sp}$	$PM_{2.5}$	Nephelometer	SFS	0.95	318	$5.3 \pm 0.1$	$-5.3 \pm 3.3$	5.01	13.45	2.98	4.82
M14	Community exposure	$B_{sp}$	$PM_{2.5}$	Nephelometer	MiniVol	0.99	10	$4.8 \pm 0.2$	$6.8 \pm 11.5$	4.81	6.75	NA	NA
MRM	Community exposure	$B_{sp}$	$PM_{2.5}$	Nephelometer	MiniVol	0.87	21	$5.4 \pm 0.7$	$78.1 \pm 33.1$	5.37	78.10	NA	NA
OLD	Community exposure	$B_{sp}$	$PM_{2.5}$	Nephelometer	MiniVol	0.93	11	$4.9 \pm 0.6$	$18.1 \pm 40.5$	4.49	18.09	NA	NA
SELM	Community exposure	$B_{sp}$	$PM_{2.5}$	Nephelometer	MiniVol	0.94	51	$6.8 \pm 0.3$	$-2.2 \pm 9.2$	5.83	46.36	4.11	4.73
SFA	Community exposure	$B_{sp}$	$PM_{2.5}$	Nephelometer	MiniVol	0.79	11	$6.0 \pm 1.6$	$4.7 \pm 36.2$	5.99	4.65	NA	NA
SOH	Community exposure	$B_{sp}$	$PM_{2.5}$	Nephelometer	MiniVol	0.91	11	$5.8 \pm 0.9$	$-7.6 \pm 38.4$	5.84	-7.61	NA	NA
VCS	Community exposure	$B_{sp}$	$PM_{2.5}$	Nephelometer	MiniVol	0.93	11	$5.2 \pm 0.7$	$26.6 \pm 44.9$	5.17	26.60	NA	NA
Average at community exposure sites						0.91	838	$5.7 \pm 0.2$	$-9.8 \pm 35.6$	5.6	13.1	2.3	9.3
ALT1	Interbasin transport	$B_{sp}$	$PM_{2.5}$	Nephelometer	MiniVol	0.95	60	$4.9 \pm 0.2$	$14.8 \pm 2.8$	4.78	18.14	NA	NA
BTI <sup>c</sup>	Interbasin transport	$B_{sp}$	$PM_{2.5}$	Nephelometer	SFS	0.96	60	$6.2 \pm 0.2$	$-2.9 \pm 6.5$	6.17	-2.29	NA	NA
LVR1	Interbasin transport	$B_{sp}$	$PM_{2.5}$	Nephelometer	MiniVol	0.96	13	$4.8 \pm 0.4$	$25.3 \pm 14.7$	4.81	25.33	NA	NA
PAC	Interbasin transport	$B_{sp}$	$PM_{2.5}$	Nephelometer	MiniVol	0.91	56	$5.2 \pm 0.3$	$16.7 \pm 3.8$	5.04	20.79	NA	NA
TEH2	Interbasin transport	$B_{sp}$	$PM_{2.5}$	Nephelometer	MiniVol	0.68	41	$5.0 \pm 0.9$	$11.3 \pm 8.8$	4.90	4.71	3.69	5.79
Average at interbasin transport sites						0.89	230	$5.3 \pm 0.4$	$10.6 \pm 5.7$	5.2	11.5	3.69	5.79
ACP	Intrabasin gradient	$B_{sp}$	$PM_{2.5}$	Nephelometer	MiniVol	NA	8	NA	NA	NA	NA	NA	NA
ANGI <sup>c</sup>	Intrabasin gradient	$B_{sp}$	$PM_{2.5}$	Nephelometer	SFS	0.83	269	$5.7 \pm 0.2$	$-10.9 \pm 6.4$	6.82	8.84	0.24	31.03
CARP	Intrabasin gradient	$B_{sp}$	$PM_{2.5}$	Nephelometer	MiniVol	0.89	20	$6.3 \pm 0.8$	$9.7 \pm 8.1$	5.48	9.67	NA	NA
EDI	Intrabasin gradient	$B_{sp}$	$PM_{2.5}$	Nephelometer	MiniVol	0.94	10	$4.4 \pm 0.6$	$65.1 \pm 43.8$	4.42	65.10	NA	NA
HELM	Intrabasin gradient	$B_{sp}$	$PM_{2.5}$	Nephelometer	MiniVol	0.87	11	$5.0 \pm 1.0$	$52.0 \pm 27.8$	5.03	52.05	NA	NA
KCW	Intrabasin gradient	$B_{sp}$	$PM_{2.5}$	Nephelometer	MiniVol	0.95	10	$4.4 \pm 0.5$	$34.9 \pm 20.1$	4.38	34.95	NA	NA
PIXL	Intrabasin gradient	$B_{sp}$	$PM_{2.5}$	Nephelometer	MiniVol	0.90	57	$5.5 \pm 0.4$	$8.3 \pm 10.5$	4.90	32.30	NA	NA
SNFH <sup>c</sup>	Intrabasin gradient	$B_{sp}$	$PM_{2.5}$	Nephelometer	SFS	0.79	64	$4.8 \pm 0.5$	$15.5 \pm 10.9$	4.87	12.28	NA	NA
SWC	Intrabasin gradient	$B_{sp}$	$PM_{2.5}$	Nephelometer	MiniVol	0.96	10	$5.1 \pm 0.5$	$40.9 \pm 20.5$	5.10	40.90	NA	NA
Average at intrabasin gradient sites						0.9	459	$5.4 \pm 0.3$	$1.6 \pm 9.4$	5.9	15.6	0.24	31.03
BODG	Boundary/background	$B_{sp}$	$PM_{2.5}$	Nephelometer	MiniVol	0.69	22	$4.9 \pm 1.1$	$39.2 \pm 19.2$	4.75	51.00	NA	NA
BRES	Source-woodburning	$B_{sp}$	$PM_{2.5}$	Nephelometer	MiniVol	0.97	11	$4.5 \pm 0.4$	$12.8 \pm 30.4$	4.52	12.82	NA	NA
FRES	Source-woodburning	$B_{sp}$	$PM_{2.5}$	Nephelometer	MiniVol	0.98	55	$5.5 \pm 0.2$	$7.0 \pm 6.6$	5.23	10.28	3.18	6.11
Average at woodburning source sites						0.97	66	$5.3 \pm 0.2$	$7.9 \pm 10.6$	5.1	10.7	3.18	6.11
FEL	Source-oilfields	$B_{sp}$	$PM_{2.5}$	Nephelometer	MiniVol	0.93	40	$4.1 \pm 0.3$	$6.2 \pm 5.0$	3.78	28.09	1.90	7.77
FELF	Source-oilfields	$B_{sp}$	$PM_{2.5}$	Nephelometer	MiniVol	0.81	38	$3.7 \pm 0.4$	$3.8 \pm 9.0$	4.42	7.29	2.55	8.16
Average at oilfield sites						0.87	78	$3.9 \pm 0.3$	$5.1 \pm 6.9$	4.1	18.0	2.2	8.0
FREM	Source-motor vehicles	$B_{sp}$	$PM_{2.5}$	Nephelometer	MiniVol	0.68	61	$3.2 \pm 0.5$	$39.5 \pm 19.5$	2.27	110.75	1.31	20.32
FEDL	Source-dairy	$B_{sp}$	$PM_{2.5}$	Nephelometer	MiniVol	0.38	29	$2.8 \pm 0.3$	$106.4 \pm 43.5$	3.65	92.15	2.39	41.81
Desert sites outside of													
CHL	SJV	$B_{sp}$	$PM_{2.5}$	Nephelometer	MiniVol	0.87	36	$4.0 \pm 0.4$	$5.4 \pm 1.2$	0.10	9.30	4.90	1.90
Desert sites outside of													
EDW	SJV	$B_{sp}$	$PM_{2.5}$	Nephelometer	MiniVol	0.55	39	$2.8 \pm 0.7$	$10.0 \pm 4.8$	1.76	12.89	0.59	17.64
Desert sites outside of													
OLW	SJV	$B_{sp}$	$PM_{2.5}$	Nephelometer	MiniVol	0.97	40	$4.1 \pm 0.2$	$0.8 \pm 1.7$	0.10	9.61	4.50	0.54
Average at desert sites outside of SJV						0.80	115	$3.6 \pm 0.4$	$5.4 \pm 2.6$	0.7	10.6	3.3	6.8

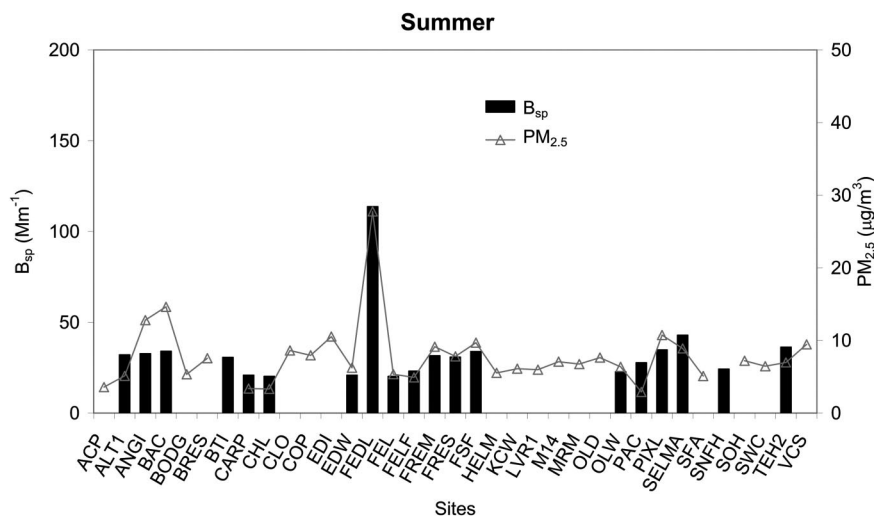
<sup>a</sup>Radiance Research M903 nephelometer (Seattle, WA); <sup>b</sup>Results from linear regression between  $B_{sp}$  (y-axis) vs  $PM_{2.5}$  mass (x-axis) for sampling periods given by Table 1; <sup>c</sup>Anchor sites.

and EDW, yielded low  $\sigma_{sp}$  of 0.1, 0.1, and 1.8 m<sup>2</sup>/g, respectively. The OLW and CHL values are not accurate owing to the higher measurement uncertainties at the low concentration levels. According to the site characteristics shown in Table 2, average wintertime  $\sigma_{sp}$  are 4.8 m<sup>2</sup>/g for background sites, 5.2 m<sup>2</sup>/g for interbasin transport sites, 5.6 m<sup>2</sup>/g for community exposure sites, and 5.9 m<sup>2</sup>/g for intrabasin gradient sites. With the exception of  $\sigma_{sp}$  at residential sites (5.1 m<sup>2</sup>/g) where home heating is

believed to be a nearby source, lower  $\sigma_{sp}$  were determined at sites near sources, including motor vehicle (2.3 m<sup>2</sup>/g), dairy farm (3.7 m<sup>2</sup>/g), and oilfield (4.1 m<sup>2</sup>/g). Most of the values are higher than the Interagency Monitoring of Protected Visual Environments (IMPROVE) dry chemical scattering efficiencies, indicating that the samples retain some liquid water, probably associated with NH<sub>4</sub>NO<sub>3</sub>, ammonium sulfate [(NH<sub>4</sub>)<sub>2</sub>SO<sub>4</sub>], and possibly with some of the organic material. The RH set point



(a)



(b)

**Figure 2.** Average  $B_{sp}$  and  $PM_{2.5}$  mass concentration at CRPAQS sites in (a) winter (February 2000, December 2000, and January 2001) and (b) summer (June 2000 to August 2000). See Table 1 for site codes.

on the nephelometer smart heater should probably have been set at a level lower than 72% to remove more of the particle liquid water. Different amounts of liquid water probably cause some of the scatter observed in the  $B_{sp}/PM_{2.5}$  comparisons.

**Seasonal Differences for Light Scattering,  $PM_{2.5}$  Mass, and Scattering Efficiencies**

Particle compositions and size distributions in the SJV have a distinct seasonal pattern.<sup>13,27-33</sup> Chow et al.<sup>28</sup> showed that  $PM_{10-2.5}$  dominates high  $PM_{10}$  levels during summer in the SJV, whereas  $PM_{2.5}$  constitutes most of the high  $PM_{10}$  concentrations during winter. During winter, shallow surface layers form under cold conditions and enhance the accumulation of carbon particles from fresh

emissions and secondary  $NH_4NO_3$ .<sup>33</sup> Coarse particles in the SJV are suppressed by periodic precipitation and fog. During CRPAQS, elevated  $PM_{2.5}$  concentrations in winter accounted for more than 50% of the annual  $PM_{2.5}$  level inside the SJV. That contribution was more pronounced in urban areas where fresh carbon emissions from vehicle exhaust and home heating can accumulate.<sup>34</sup>

Figures 2a and 2b also show that average  $B_{sp}$  and  $PM_{2.5}$  mass were higher during winter than summer. In summer, the dairy farm (FEDL) site had the highest  $PM_{2.5}$  (27.9  $\mu g/m^3$ ). Elevated  $PM_{2.5}$  levels at the FEDL site were also found during winter (38.6  $\mu g/m^3$ ) and occurred throughout the year. These high levels were not reflected at nearby monitors, indicating that the zone of influence for this source was small.<sup>34</sup>

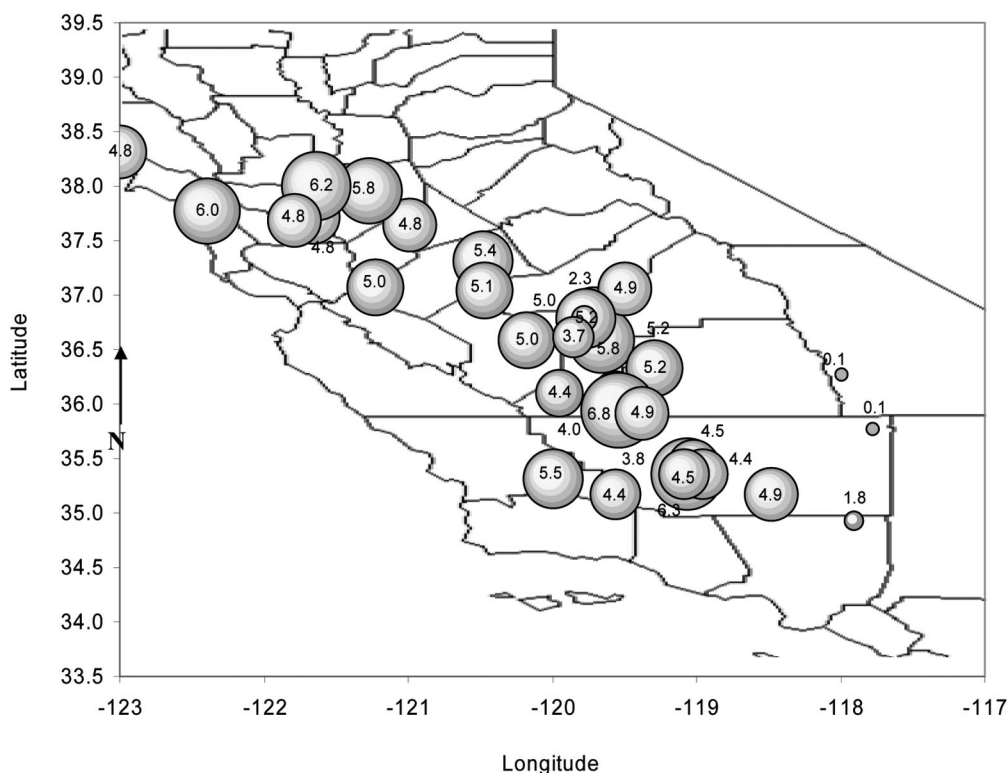


**Figure 3.** Spatial variation of  $\sigma_{sp}$  ( $m^2/g$ ) averaged over winter sampling periods (the diameter of the circle is proportional to  $\sigma_{sp}$  except for the easternmost desert sites).

Winter and summer  $\sigma_{sp}$  as a function of  $PM_{2.5}$  mass is shown in Figure 4. The average  $\sigma_{sp}$  was  $2.6 m^2/g$  in summer and  $4.6 m^2/g$  in winter, consistent with differences in particle composition, particle size, and RH that affect  $\sigma_{sp}$ . Suspended dust events are more common during summer, owing to drier conditions and more agricultural activity. Higher summertime  $\sigma_{sp}$  at the OLW and CHL sites is influenced by the outflow of  $PM_{2.5}$  from the SJV and

from the South Coast Air Basin that provides a larger fraction of  $PM_{2.5}$  than during winter, when such outflow is suppressed.<sup>35,36</sup>

Daily average  $B_{sp}$  and  $PM_{2.5}$  at the regional-scale ANGI and urban-scale BAC sites in winter and summer are shown in Figures 5a and 5b, respectively. Both sites display a similar seasonal dependence of  $B_{sp}$  on  $PM_{2.5}$  (i.e., higher scattering efficiency and correlation during winter

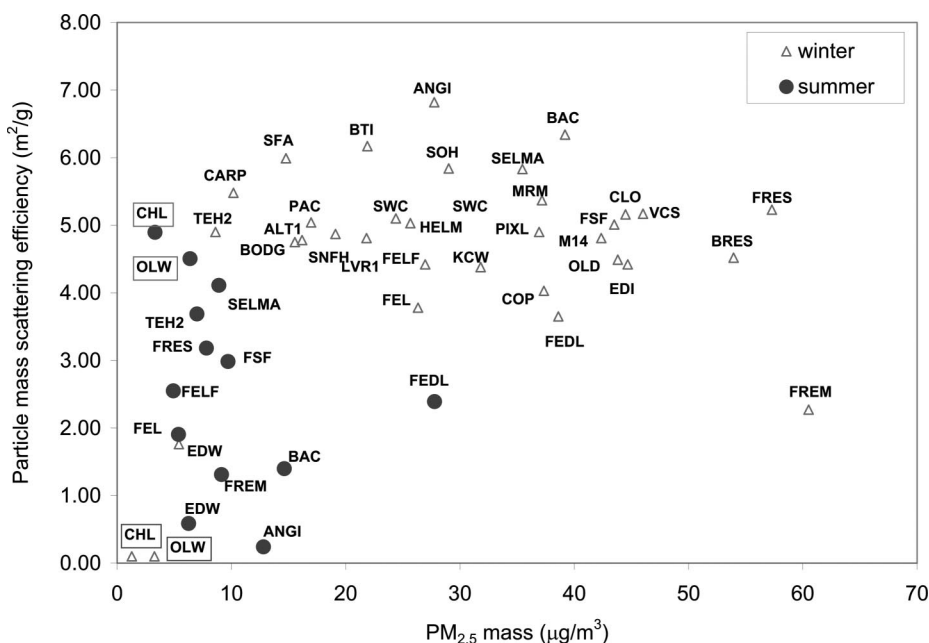


**Figure 4.**  $\sigma_{sp}$  during winter and summer.

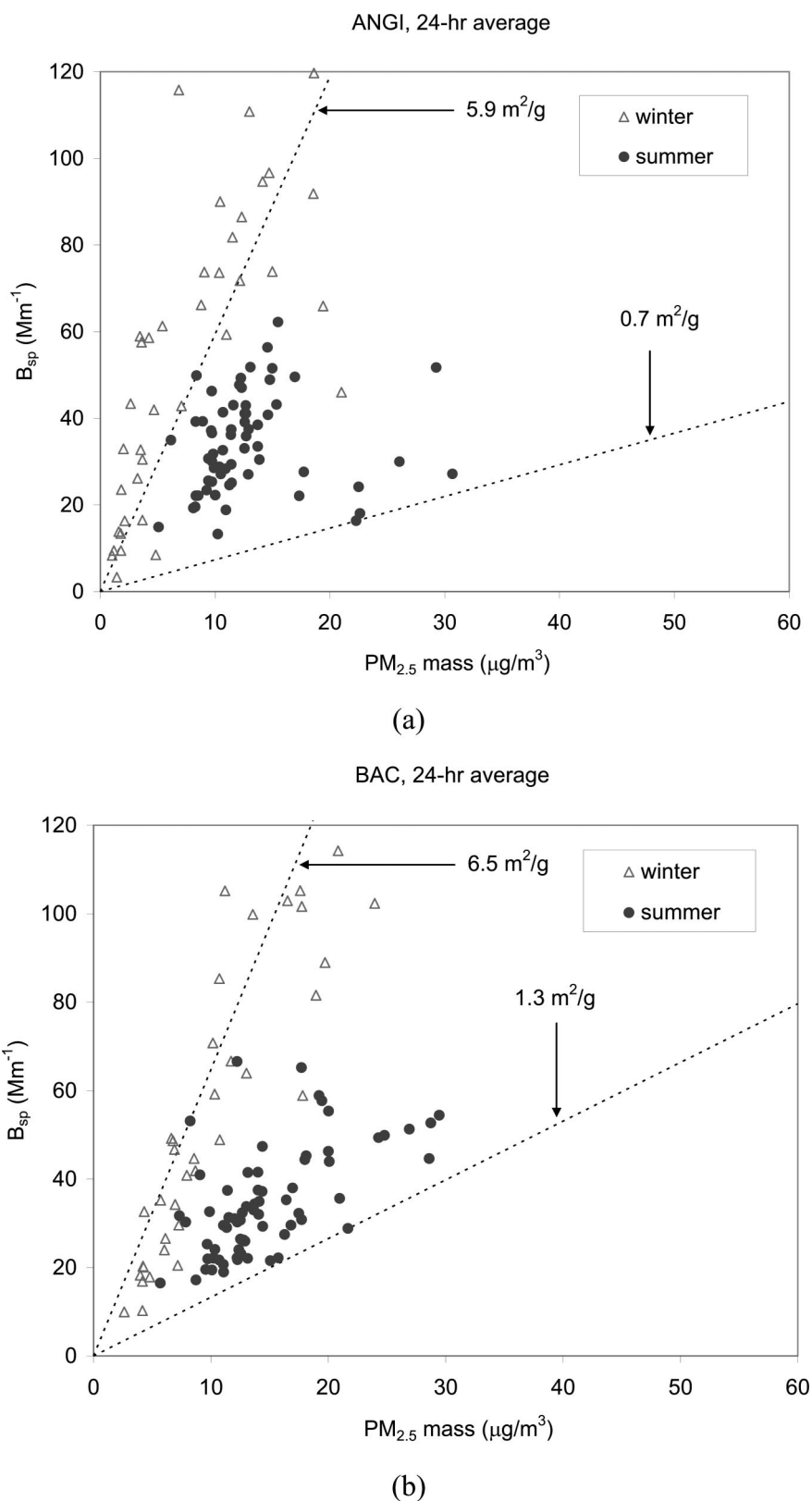


**Figure 5.** Daily average  $B_{sp}$  and  $PM_{2.5}$  mass at the (a) ANGI and (b) BAC sites during winter and summer.

than during summer). Summertime  $\sigma_{sp}$  varied widely from  $0.7 \text{ m}^2/\text{g}$  to  $5.9 \text{ m}^2/\text{g}$  at ANGI and from  $1.3 \text{ m}^2/\text{g}$  to  $6.5 \text{ m}^2/\text{g}$  at BAC. Wintertime relationships are much more consistent.

When an all-site and both-season average of  $\sigma_{sp} = 4.9 \text{ m}^2/\text{g}$  is used to estimate  $PM_{2.5}$  mass from  $B_{sp}$ , the slope between the estimated and measured  $PM_{2.5}$  mass deviates from a 1:1 line, especially during the summer

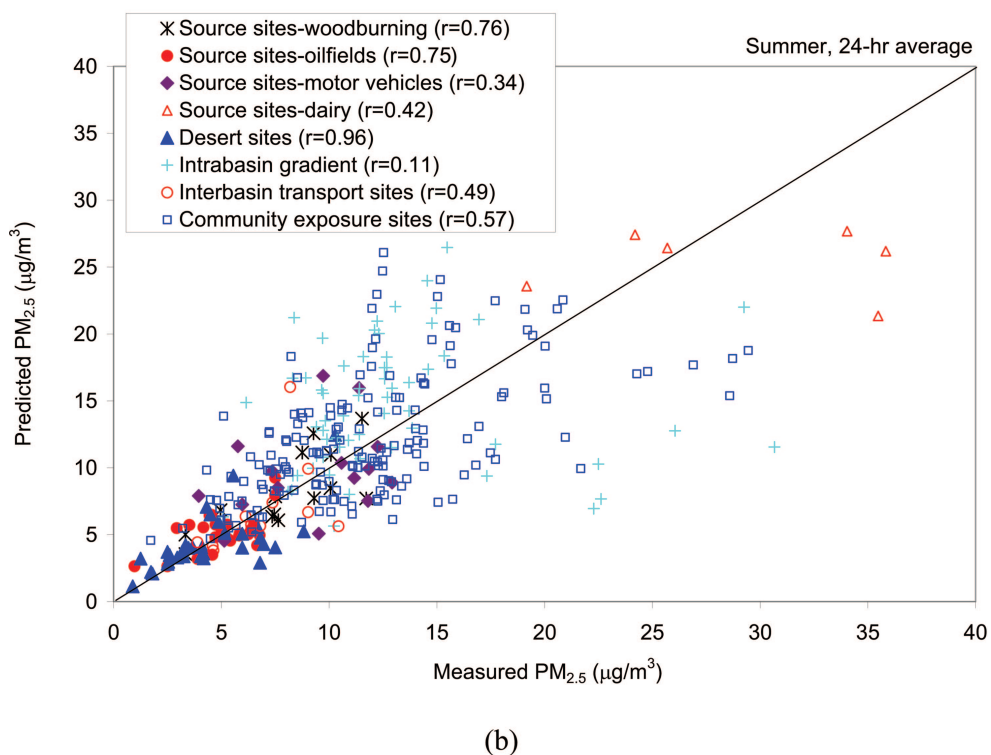
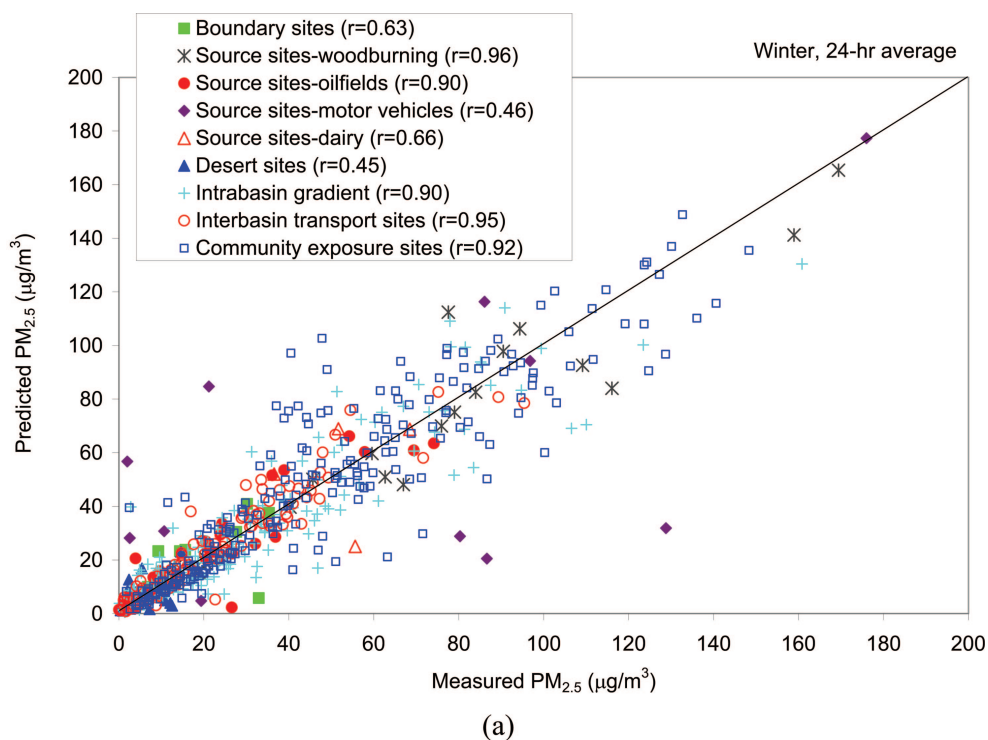


**Figure 6.** Comparison of PM<sub>2.5</sub> mass estimated from B<sub>sp</sub> and measured PM<sub>2.5</sub> mass at different types of sites during (a) winter and (b) summer using site-type specific  $\sigma_{sp}$ . Correlation coefficients (r) between estimated and measured PM<sub>2.5</sub> are given in the legend for each site type.

(slope = 0.36). This average B<sub>sp</sub> does not accurately estimate PM<sub>2.5</sub> mass everywhere all the time. Figures 6a and 6b compare PM<sub>2.5</sub> estimated from B<sub>sp</sub> with the measured PM<sub>2.5</sub> mass at different types of sites in winter and summer, respectively, showing closer agreement

when site-type and seasonal  $\sigma_{sp}$  values are used. Community exposure and interbasin gradient/transport sites, as well as source-dominated home heating and oilfield sites, show correlations exceeding 0.9 during winter. Correlations are low during summer, with the

**Table 3.** Comparison of particle light scattering and PM<sub>2.5</sub> at the FSF for data acquired between September 1, 2000, and August 31, 2001.

Sampling period	Observables		Measurement methods		y		x		Slope ± Standard Error (m <sup>2</sup> /g)	Intercept ± Standard Error (m <sup>2</sup> /g)
	y	x	y	x	Average ± std (Mm <sup>-1</sup> )	Average ± std (Mm <sup>-1</sup> )	Corr. (r)	N		
Winter <sup>a</sup>	B <sub>sp</sub>	PM <sub>2.5</sub>	Radiance nephelometer TSP <sup>a</sup>	BAM	334.7 ± 233.4	70.0 ± 47.6	0.96	1524	4.50 ± 0.03	10.51 ± 2.69
Summer <sup>b</sup>	B <sub>sp</sub>	PM <sub>2.5</sub>	Radiance nephelometer TSP	BAM	21.9 ± 20.7	12.4 ± 8.2	0.84	1895	1.72 ± 0.03	0.41 ± 0.38
Winter	B <sub>sp</sub>	PM <sub>2.5</sub>	Radiance nephelometer TSP	TEOM	334.7 ± 233.4	27.7 ± 24.4	0.88	1546	8.79 ± 0.12	103.58 ± 4.31
Summer	B <sub>sp</sub>	PM <sub>2.5</sub>	Radiance nephelometer TSP	TEOM	21.9 ± 20.7	9.0 ± 4.7	0.74	639	2.17 ± 0.08	-2.05 ± 0.80
Winter	B <sub>sp</sub>	PM <sub>2.5</sub>	Radiance nephelometer TSP	DustTrak	334.7 ± 233.4	82.7 ± 61.3	0.96	1079	2.14 ± 0.02	-8.71 ± 2.29
Summer	B <sub>sp</sub>	PM <sub>2.5</sub>	Radiance nephelometer TSP	DustTrak	21.9 ± 20.7	30.5 ± 20.7	0.61	1857	0.52 ± 0.02	6.89 ± 0.59
Winter	B <sub>sp</sub>	PM <sub>2.5</sub>	Radiance nephelometer TSP	GreenTek	334.7 ± 233.4	84.1 ± 54.7	0.82	798	2.66 ± 0.07	85.22 ± 6.54
Summer	B <sub>sp</sub>	PM <sub>2.5</sub>	Radiance nephelometer TSP	GreenTek	21.9 ± 20.7	7.7 ± 7.6	0.79	1777	2.24 ± 0.04	6.79 ± 0.46
Winter	B <sub>sp</sub>	PM <sub>2.5</sub>	Radiance nephelometer TSP	FRM filter	333.4 ± 200.1	78.0 ± 47.2	0.97	10	4.80 ± 0.45	-0.05 ± 40.30
Summer	B <sub>sp</sub>	PM <sub>2.5</sub>	Radiance nephelometer TSP	FRM filter	21.9 ± 20.7	8.5 ± 3.1	0.92	13	3.48 ± 0.44	-9.87 ± 4.00
Winter	B <sub>spf</sub>	PM <sub>2.5</sub>	Radiance nephelometer PM <sub>2.5</sub>	BAM	301.0 ± 223.3	70.0 ± 47.6	0.97	1391	4.30 ± 0.03	5.13 ± 2.48
Summer	B <sub>spf</sub>	PM <sub>2.5</sub>	Radiance nephelometer PM <sub>2.5</sub>	BAM	22.6 ± 21.4	12.4 ± 8.2	0.86	1800	1.78 ± 0.03	-0.16 ± 0.38
Winter	B <sub>spf</sub>	PM <sub>2.5</sub>	Radiance nephelometer PM <sub>2.5</sub>	TEOM	301.0 ± 223.3	27.7 ± 24.4	0.89	1412	8.50 ± 0.12	85.38 ± 4.13
Summer	B <sub>spf</sub>	PM <sub>2.5</sub>	Radiance nephelometer PM <sub>2.5</sub>	TEOM	22.6 ± 21.4	9.0 ± 4.7	0.75	580	2.32 ± 0.08	-2.51 ± 0.88
Winter	B <sub>spf</sub>	PM <sub>2.5</sub>	Radiance nephelometer PM <sub>2.5</sub>	DustTrak	301.0 ± 223.3	82.7 ± 61.3	0.96	1035	2.04 ± 0.02	-12.38 ± 2.11
Summer	B <sub>spf</sub>	PM <sub>2.5</sub>	Radiance nephelometer PM <sub>2.5</sub>	DustTrak	22.6 ± 21.4	30.5 ± 20.7	0.64	1753	0.56 ± 0.02	6.60 ± 0.61
Winter	B <sub>spf</sub>	PM <sub>2.5</sub>	Radiance nephelometer PM <sub>2.5</sub>	GreenTek	301.0 ± 223.3	84.1 ± 54.7	0.83	776	2.63 ± 0.06	70.07 ± 6.22
Summer	B <sub>spf</sub>	PM <sub>2.5</sub>	Radiance nephelometer PM <sub>2.5</sub>	GreenTek	22.6 ± 21.4	7.7 ± 7.6	0.81	1718	2.34 ± 0.04	6.26 ± 0.46
Winter	B <sub>spf</sub>	PM <sub>2.5</sub>	Radiance nephelometer PM <sub>2.5</sub>	FRM filter	316.8 ± 196.7	78.0 ± 47.2	0.97	10	4.67 ± 0.41	-5.97 ± 36.71
Summer	B <sub>spf</sub>	PM <sub>2.5</sub>	Radiance nephelometer PM <sub>2.5</sub>	FRM filter	22.6 ± 21.4	8.5 ± 3.1	0.94	13	3.57 ± 0.40	-10.18 ± 3.59
Winter	B <sub>sp</sub>	PM <sub>2.5</sub>	Radiance nephelometer TSP	PM <sub>2.5</sub> BAM	334.7 ± 233.4	58.4 ± 34.5	0.96	1527	4.54 ± 0.03	12.13 ± 2.69
		PM <sub>10-2.5</sub>		PM <sub>10-2.5</sub> BAM <sup>d</sup>		9.2 ± 9.6			-0.65 ± 0.16	
Summer	B <sub>sp</sub>	PM <sub>2.5</sub>	Radiance nephelometer TSP	PM <sub>2.5</sub> BAM	21.9 ± 20.7	9.7 ± 3.9	0.85	1891	1.63 ± 0.03	-2.26 ± 0.46
		PM <sub>10-2.5</sub>		PM <sub>10-2.5</sub> BAM <sup>d</sup>		29.5 ± 11.1			0.13 ± 0.01	
Winter	B <sub>sp</sub>	PM <sub>2.5</sub>	Radiance nephelometer TSP	PM <sub>2.5</sub> TEOM	334.7 ± 233.4	22.1 ± 17.7	0.84	937	8.99 ± 0.20	102.10 ± 5.50
		PM <sub>10-2.5</sub>		PM <sub>10-2.5</sub> TEOM <sup>e</sup>		4.8 ± 6.1			-2.27 ± 0.58	
Summer	B <sub>sp</sub>	PM <sub>2.5</sub>	Radiance nephelometer TSP	PM <sub>2.5</sub> TEOM	21.9 ± 20.7	9.0 ± 4.8	0.74	639	2.15 ± 0.09	-2.12 ± 0.82
		PM <sub>10-2.5</sub>		PM <sub>10-2.5</sub> TEOM <sup>e</sup>		18.2 ± 13.0			0.01 ± 0.03	
Winter	B <sub>sp</sub>	B <sub>sp</sub>	NGN2 nephelometer TSP	Radiance nephelometer TSP	410.4 ± 269.4	265.1 ± 181.0	0.92	1117	1.38 ± 0.02	45.62 ± 5.46
Summer	B <sub>sp</sub>	B <sub>sp</sub>	NGN2 nephelometer TSP	Radiance nephelometer TSP	18.8 ± 6.4	21.9 ± 20.7	0.94	2001	0.29 ± 0.00	12.52 ± 0.07
Winter	B <sub>sp</sub>	B <sub>spf</sub>	Radiance nephelometer TSP	Radiance nephelometer PM <sub>2.5</sub>	333.4 ± 200.1	301.0 ± 223.3	1.00	1427	1.04 ± 0.00	5.11 ± 0.56
Summer	B <sub>sp</sub>	B <sub>spf</sub>	Radiance nephelometer TSP	Radiance nephelometer PM <sub>2.5</sub>	21.9 ± 20.7	22.6 ± 21.4	1.00	2032	0.98 ± 0.00	0.16 ± 0.06

<sup>a</sup>Winter (December 2000 to February 2001); <sup>b</sup>Summer (June 2001 to August 2001); <sup>c</sup>B<sub>sp</sub> from a Radiance Research M903 Nephelometer (Seattle, WA) without a size-selective inlet, presumably measuring total suspended particles (TSP, particles with aerodynamic diameters < ~30 μm) scattering; <sup>d</sup>Multiple linear regression with the B<sub>sp</sub> as the dependent variable, and PM<sub>2.5</sub> and PM<sub>10-2.5</sub> concentrations as the independent variables; <sup>e</sup>Multiple linear regression with the B<sub>sp</sub> as the dependent variable, and PM<sub>2.5</sub> and PM<sub>10-2.5</sub> concentrations as the independent variables; <sup>f</sup>1-hr average data were used for comparisons, except for the FRM filter mass (24-hr average). The average value was calculated over the collocated sampling period for each instrument.

exception of the desert sites, indicating that B<sub>sp</sub> is a less reliable estimator of PM<sub>2.5</sub> during that season.

B<sub>sp</sub> was compared with PM<sub>10</sub> mass for a neighborhood-scale study centered on the Corcoran (COP) site from October 10, 2000, to November 14, 2000, to determine how well B<sub>sp</sub> in the area is related to PM<sub>10</sub>. B<sub>sp</sub> and PM<sub>10</sub> were not as well correlated (r = 0.66) and yielded smaller σ<sub>sp</sub> (2.6 m<sup>2</sup>/g) than those found for B<sub>sp</sub> and PM<sub>2.5</sub> (r = 0.89, 4.5 m<sup>2</sup>/g). This reflects the lower scattering efficiency expected for the coarse particles. IMPROVE estimates a coarse particle mass scattering efficiency (σ<sub>spc</sub>) of 0.6 m<sup>2</sup>/g.<sup>13</sup>

#### Light Scattering and PM Comparisons at FSF

B<sub>spf</sub> derived from the Fresno PM<sub>2.5</sub> nephelometer and B<sub>sp</sub> from other instruments are compared with PM<sub>2.5</sub> mass

from different instruments in Table 3. The correlations between hourly averaged B<sub>spf</sub> and PM<sub>2.5</sub> BAM are higher during winter (r = 0.97) than during summer (r = 0.85) with 2-fold higher PM<sub>2.5</sub> σ<sub>sp</sub> during winter (4.3 m<sup>2</sup>/g) than during summer (1.8 m<sup>2</sup>/g), as shown in Figure 7. B<sub>sp</sub> and B<sub>spf</sub> measured with the Radiance nephelometers were highly correlated (Table 3), with a higher regression slope in winter than summer (1.04 versus 0.98). Coarse particles appear to have a small effect on the B<sub>sp</sub> measurement.

Results from a multiple linear regression with B<sub>sp</sub> as the dependent variable and PM<sub>2.5</sub> and PM<sub>10-2.5</sub> concentrations as the independent variables (i.e., B<sub>sp</sub> = intercept + σ<sub>spf</sub> × PM<sub>2.5</sub> mass + σ<sub>spc</sub> [coarse (PM<sub>10-2.5</sub>) particle mass scattering efficiency] × PM<sub>10-2.5</sub> mass) are also included in Table 3. For all but the wintertime comparison with the TEOM, the σ<sub>spc</sub> is negligible for these samples. PM<sub>2.5</sub> and

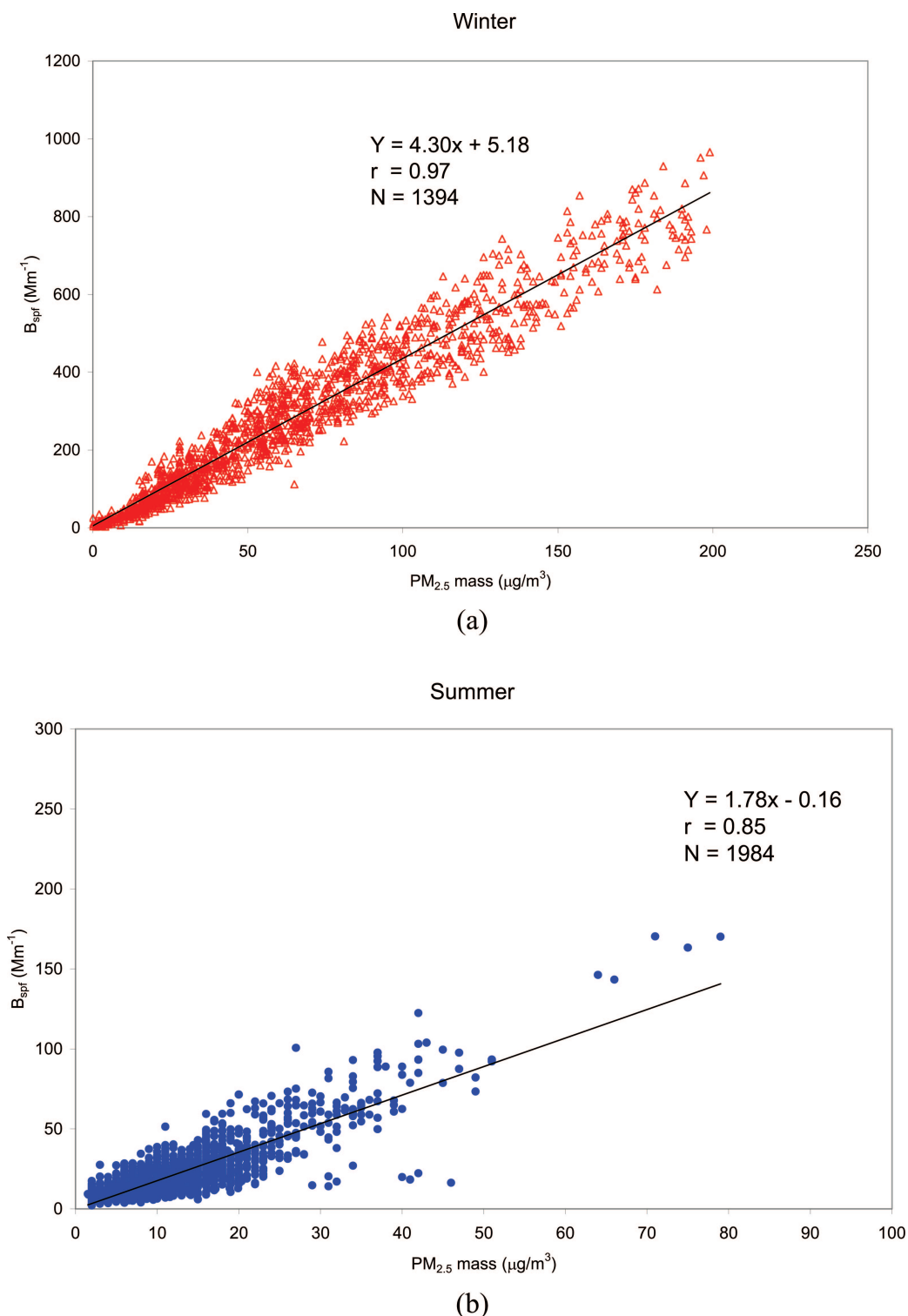


**Figure 7.** Comparison of hourly average  $B_{\text{spf}}$  from a Radiance Research M903 nephelometer with a  $\text{PM}_{2.5}$  size-selective inlet and  $\text{PM}_{2.5}$  mass determined by BAM at the FSF during (a) winter and (b) summer.

$\text{PM}_{10-2.5}$  concentrations are often correlated at Fresno, but the  $\sigma_{\text{spf}}$  and  $\sigma_{\text{spc}}$  are not necessarily constant. This results in some uncertainties, even negative values, for the multiple linear regression coefficients, especially for the TEOM measurements during summer.

On average,  $B_{\text{sp}}$  from the NGN2 ambient temperature nephelometer ( $410 \text{ Mm}^{-1}$ ) was 1.6 times  $B_{\text{sp}}$  from the Radiance nephelometer ( $265 \text{ Mm}^{-1}$ ) during the winter, which is expected, owing to the higher RH. This comparison indicates that water is being removed in the Radiance

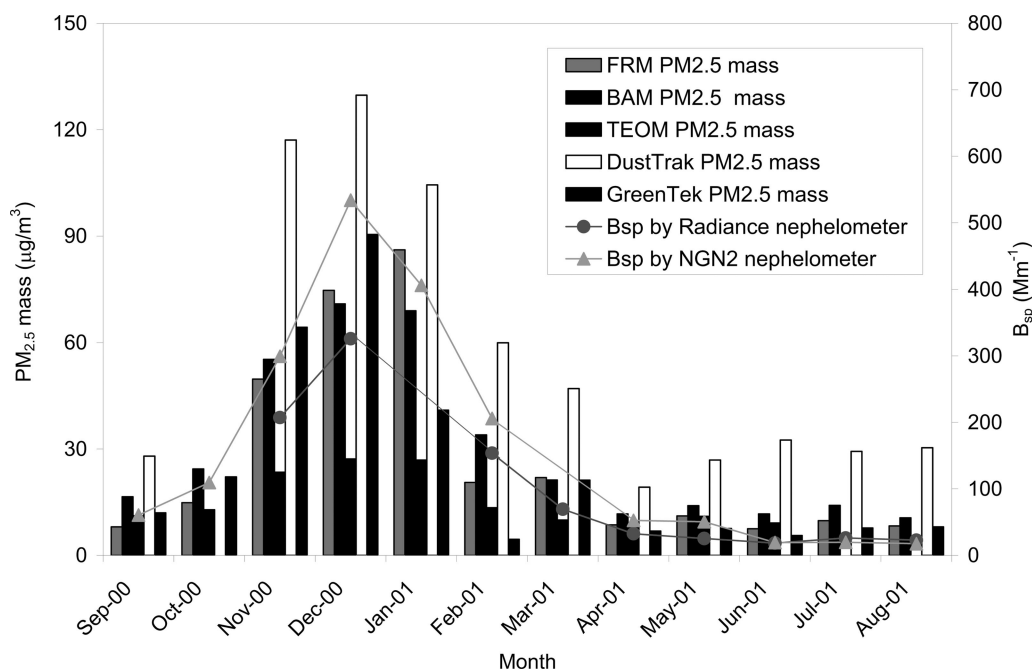


**Figure 8.** Monthly average  $B_{sp}$  by Radiance Research M903 and OPTEC NGN2 nephelometers and  $PM_{2.5}$  mass concentrations determined by  $PM_{2.5}$  FRM filter sampler, BAM, TEOM, DustTrak photometer, and GreenTek photometer at the FSF from September 2000 to August 2001.

nephelometer by the smart heater. During summer when RH was much lower than winter, average NGN2  $B_{sp}$  ( $19 \text{ Mm}^{-1}$ ) was comparable to Radiance  $B_{sp}$  ( $22 \text{ Mm}^{-1}$ ). After excluding  $B_{sp}$  values  $> 1000 \text{ Mm}^{-1}$  from the NGN2 dataset, correlations with the Radiance  $B_{sp}$  nephelometer ranged from 0.92 to 0.94.

The monthly average  $B_{sp}$  determined by the Radiance and OPTEC NGN2 nephelometers and  $PM_{2.5}$  mass concentrations determined by the FRM, BAM, TEOM, DustTrak, and GreenTek are compared in Figure 8. During the

winter,  $PM_{2.5}$  TEOM was lower because of evaporation of  $NH_4NO_3$  at its  $50 \text{ }^\circ\text{C}$  internal temperature.<sup>37-39</sup> The filter dynamic measurement system<sup>40</sup> quantifies TEOM evaporation, but this was not implemented at the FSF. Among all measurements, the two photometers consistently reported higher  $PM_{2.5}$  mass. On average, the DustTrak reported 2.2 and 4.3 times higher  $PM_{2.5}$  mass in winter and summer, respectively, than the GreenTek.

Figures 9a and 9b show similar diurnal variations between  $B_{spf}$  and  $PM_{2.5}$  mass at FSF. Although these are

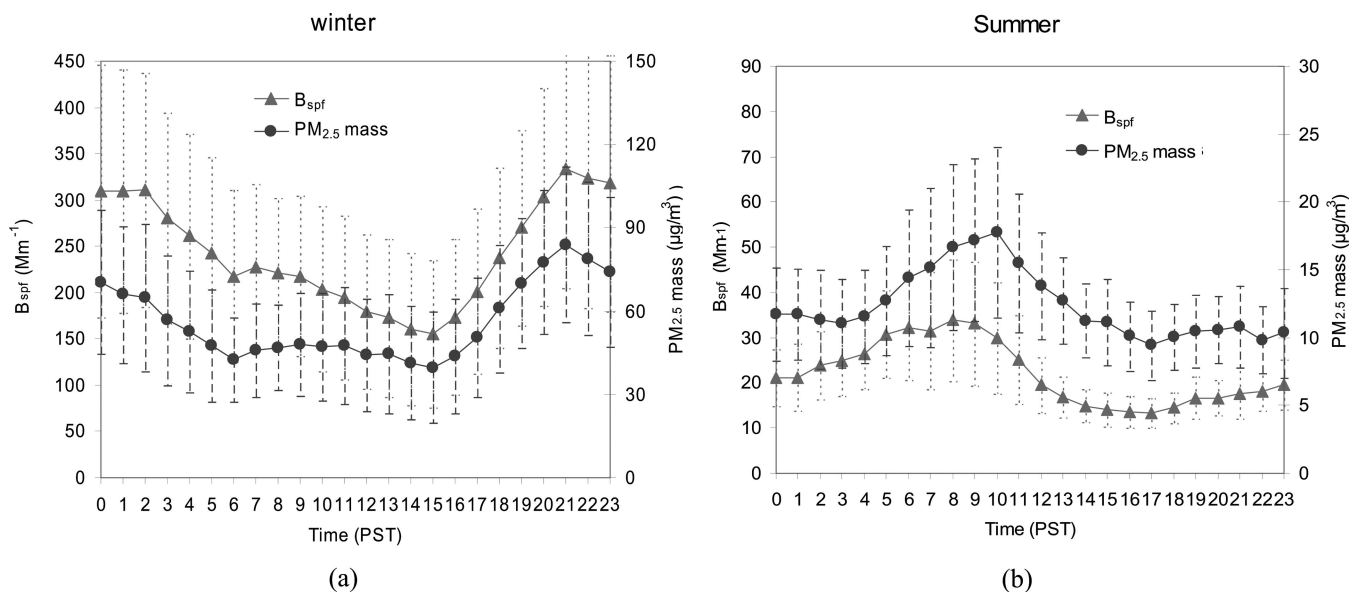


**Figure 9.** Diurnal variations of  $B_{spf}$  determined by the Radiance Research M903 nephelometer with a  $PM_{2.5}$  size-selective inlet and  $PM_{2.5}$  mass concentration determined by BAM, averaged by the time of day at the FSF during (a) winter and (b) summer.

average values, examination of individual days shows that they track each other in most situations. This comparison supports the use of  $PM_{2.5}$  derived from  $B_{sp}$  to better understand  $PM_{2.5}$  variability within a 24-hr period at sites that do not have all of the Supersite instrumentation.

## CONCLUSION

Site-type and season-specific  $PM_{2.5}$   $\sigma_{sp}$  can be applied to  $B_{sp}$  measurements from a nephelometer to estimate  $PM_{2.5}$  concentrations with reasonable accuracy and precision in California's San Joaquin Valley. Periodic heating of the nephelometer inlet to obtain RH below a certain value (probably <60%) can be applied to remove liquid water while minimizing evaporation of volatile compounds such as  $NH_4NO_3$ . Best agreements between  $B_{sp}$  and  $PM_{2.5}$  are found during winter and for sites that are not located near sources. Summertime  $\sigma_{sp}$  were lower owing to drier conditions with less hygroscopic  $NH_4NO_3$  and a larger proportion of soil-related PM, all of which result in lower  $\sigma_{sp}$ .

## ACKNOWLEDGMENTS

This work was supported by the CRPAQS under the management of the California Air Resources Board and U.S. Environmental Protection Agency under Contract #R-82805701 for the Fresno Supersite. The conclusions are those of the authors and do not necessarily reflect the views of the sponsoring agencies. Any mention of commercially available products and supplies does not constitute an endorsement of these products and supplies. The authors thank Jo Gerrard and Tim Richard of DRI for assembling and editing the manuscript.

## REFERENCES

- Beuttell, R.G.; Brewer, A.W. Instruments for the Measurement of the Visual Range; *J. Sci. Instrum.* **1949**, *26*, 357-359.
- Ahlquist, N.C.; Charlson, R.J. A New Instrument for Evaluating the Visual Quality of Air; *J. Air Pollut. Control Assoc.* **1967**, *17*, 467-469.
- Ruby, M.G.; Rood, M.J.; Chow, J.C.; Egami, R.T.; Rogers, C.F.; Watson, J.G. Integrating Nephelometer Measurement of Scattering Coefficient and Fine Particle Concentrations. In *Methods of Air Sampling and Analysis*, 3rd ed.; Lodge, J.P., Ed.; Lewis: Chelsea, MI, 1989; pp. 450-457.
- Brauer, M. Assessment of Indoor Aerosols with an Integrating Nephelometer; *J. Expo. Anal. Environ. Epidemiol.* **1995**, *5*, 45-56.
- Charlson, R.J.; Ahlquist, N.C.; Horvath, H. On the Generality of Correlation of Atmospheric Aerosol Mass Concentration and Light Scatter; *Atmos. Environ.* **1968**, *2*, 455-464.
- Chow, J.C.; Watson, J.G.; Lowenthal, D.H.; Richards, L.W. Comparability between  $PM_{2.5}$  and Light Scattering Measurements; *Environmental Monitoring and Assessment*, **2002**, *79*, 29-45.
- Lewis, C.W. On the Proportionality of Fine Mass Concentration and Extinction Coefficient for Bimodal Size Distributions; *Atmos. Environ.* **1981**, *15*, 2639-2646.
- Scheff, P.A.; Wadden, R.A. Comparisons of Three Methods of Particulate Measurements in Chicago Air; *Atmos. Environ.* **1979**, *16*, 639-643.
- Sioutas, C.; Kim, S.; Chang, M.C.; Terrell, L.L.; Gong, H. Field evaluation of a modified DataRAM MIE Scattering Monitor for Real-Time  $PM_{2.5}$  Mass Concentration Measurements; *Atmos. Environ.* **2000**, *34*, 4829-4838.
- Thielke, J.F.; Charlson, R.J.; Winter, J.W.; Ahlquist, N.C.; Whitby, K.T.; Husar, R.B.; Liu, B.Y.H. Multiwavelength Nephelometer Measurements in Los Angeles Smog Aerosols. II. Correlation with Size Distributions, Volume Concentrations; *J. Colloid Interface Sci.* **1972**, *39*, 252-259.
- Thomas, A.; Gebhart, J. Correlations between Gravimetry and Light Scattering Photometry for Atmospheric Aerosols; *Atmos. Environ.* **1994**, *28*, 935-938.
- Waggoner, A.P.; Weiss, R.E. Comparison of Fine Particle Mass Concentration and Light Scattering Extinction in Ambient Aerosol; *Atmos. Environ.* **1980**, *14*, 623-626.
- Watson, J.G. Visibility: Science and Regulation; *J. Air & Waste Manage. Assoc.* **2002**, *52*, 628-713.
- Ensor, D.S.; Waggoner, A.P. Angular Truncation Error in the Integrating Nephelometer; *Atmos. Environ.* **1970**, *4*, 481-487.
- Ensor, D.S.; Pilat, M.J. The Effect of Particle Size Distribution on Light Transmittance Measurement; *J. Am. Ind. Hyg. Assoc.* **1971**, *32*, 287-292.
- Guyon, P.; Graham, B.; Beck, J.; Boucher, O.; Gerasopoulos, E.; Mayol-Bracero, O.L.; Roberts, G.C.; Artaxo, P.; Andreae, M.O. Physical Properties and Concentrations of Aerosol Particles Over the Amazon Tropical Forest During Background and Biomass Burning Conditions; *Atmos. Chem. Physics Discussion*, **2003**, *3*, 1333-1366.
- Moosmüller, H.; Arnott, W.P. Angular Truncation Errors in Integrating Nephelometry; *Rev. Sci. Instrum.* **2003**, *74*, 3492-3501, doi:10.1063/1.1581355.
- Quenzel, H.; Ruppertsberg, G.H.; Schellhase, R. Calculations about the Systematic Error of Visibility-Meters Measuring Scattered Light; *Atmos. Environ.* **1975**, *9*, 587-601.
- Rabinoff, R.A.; Herman, B.M. Effect of Aerosol Size Distribution on the Accuracy of the Integrating Nephelometer; *J. Appl. Meteorol.* **1973**, *12*, 184-186.
- Rosen, J.M.; Pinnick, R.G.; Garvey, D.M. Nephelometer Optical Response Model for the Interpretation of Atmospheric Aerosol Measurements; *Appl. Opt.* **1997**, *36*, 2642-2649.
- Varma, R.; Moosmüller, H.; Arnott, W.P. Toward an Ideal Integrating Nephelometer; *Opt. Lett.* **2003**, *28*, 1007-1009.
- Watson, J.G.; DuBois, D.W.; DeMandel, R.; Kaduwela, A.P.; Magliano, K.L.; McDade, C.; Mueller, P.K.; Ranzieri, A.J.; Roth, P.M.; Tanrikulu, S. *Field Program Plan for the California Regional  $PM_{2.5}/PM_{10}$  Air Quality Study (CRPAQS)*; Prepared for California Air Resources Board, Sacramento, CA, by Desert Research Institute: Reno, NV, 1998.
- Richards, L.W.; Weiss, R.E.; Waggoner, A.P. Radiance Research Model 903 Integrating Nephelometer. In *Proceedings, Regional Haze and Global Radiation Balance—Aerosol Measurements and Models: Closure, Reconciliation and Evaluation*; A&WMA: Pittsburgh, PA, 2001, 3B7-1-3B7-5.
- Richards, L.W.; Lehrman, D.E.; Weiss, R.E.; Bush, D.; Watson, J.G.; McDade, C.E.; Magliano, K. Light Scattering Measurements during the California Regional  $PM_{10}/PM_{2.5}$  Air Quality Study. In *Proceedings, Regional Haze and Global Radiation Balance - Aerosol Measurements and Models: Closure, Reconciliation and Evaluation*; A&WMA: Pittsburgh, PA, 2001, 5A2-1-5A2-5.
- Alcorn, S.H.; Richards, L.W.; Lehrman, D.E. *Comparisons Between Light Scattering and Fine Particle Mass Data*; STI-90232102644; Prepared for California Air Resources Board, Sacramento, CA, by Sonoma Technology, Inc.: Petaluma, CA, 2004.
- Baldauf, R.W.; Lane, D.D.; Marotz, G.A.; Wiener, R.W. Performance evaluation of the Portable MiniVol Particulate Matter Sampler; *Atmos. Environ.* **2001**, *35*, 6087-6091.
- Watson, J.G.; Chow, J.C.; Bowen, J.L.; Lowenthal, D.H.; Hering, S.; Ouchida, P.; Oslund, W. Air quality Measurements from the Fresno Supersite; *J. Air & Waste Manage. Assoc.* **2000**, *50*, 1321-1334.
- Chow, J.C.; Watson, J.G.; Lowenthal, D.H.; Solomon, P.A.; Magliano, K.L.; Ziman, S.D.; Richards, L.W.  $PM_{10}$  and  $PM_{2.5}$  Compositions in California's San Joaquin Valley; *Aerosol Sci. Technol.* **1993**, *18*, 105-128.
- Watson, J.G.; Chow, J.C.; Park, K.; Lowenthal, D.H. Nanoparticle and Ultrafine Particle Events at the Fresno Supersite; *J. Air & Waste Manage. Assoc.* in press.
- Chow, J.C.; Watson, J.G.; Lowenthal, D.H.; Solomon, P.A.; Magliano, K.L.; Ziman, S.D.; Richards, L.W.  $PM_{10}$  Source Apportionment in California's San Joaquin Valley; *Atmos. Environ.* **1992**, *26A*, 3335-3354.
- Chow, J.C.; Watson, J.G.; Lu, Z.; Lowenthal, D.H.; Frazier, C.A.; Solomon, P.A.; Thuillier, R.H.; Magliano, K.L. Descriptive analysis of  $PM_{2.5}$  and  $PM_{10}$  at Regionally Representative Locations during SJAQS/AUSPEX; *Atmos. Environ.* **1996**, *30*, 2079-2112.
- Chow, J.C.; Watson, J.G.; Lowenthal, D.H.; Hackney, R.; Magliano, K.L.; Lehrman, D.; Smith, T. Temporal Variations of  $PM_{2.5}$ ,  $PM_{10}$ , and Gaseous Precursors during the 1995 Integrated Monitoring Study in Central California; *J. Air & Waste Manage. Assoc.* **1999**, *49(PM)*, PM16-PM24.
- Watson, J.G.; Chow, J.C. A Wintertime  $PM_{2.5}$  Episode at the Fresno, CA Supersite; *Atmos. Environ.* **2002**, *36*, 465-475.
- Chow, J.C.; Watson, J.G.; Chen, L.W.A.  $PM_{2.5}$  Chemical Composition and Spatiotemporal Variability during the California Regional  $PM_{10}/PM_{2.5}$  Air Quality Study (CRPAQS); *J. Geophys. Res.* in press.
- White, W.H.; Macias, E.S. Chemical Mass Balancing with Ill Defined Sources: Regional Apportionment in the California Desert; *Atmos. Environ.* **1991**, *25A*, 1547-1557.
- Green, M.C.; Flocchini, R.G.; Myrup, L.O. The relationship of the Extinction Coefficient Distribution to Wind Field Patterns in Southern California; *Atmos. Environ.* **1992**, *26A*, 827-840.

37. Jaques, P.A.; Ambs, J.L.; Grant, W.L.; Sioutas, C. Field Evaluation of the Differential TEOM Monitor for Continuous PM<sub>2.5</sub> Mass Concentrations; *Aerosol Sci. Technol.* **2004**, *38*(Suppl. 1), 49-59.
38. Hitznerberger, R.; Berner, A.; Galambos, Z.; Maenhaut, W.; Cafmeyer, J.; Schwarz, J.; Muller, K.; Spindler, G.; Wieprecht, W.; Acker, K.; Hillamo, R.; Makela, T. Intercomparison of Methods to Measure the Mass Concentration of the Atmospheric Aerosol during INTERCOMP2000—Influence of Instrumentation and Size Cuts; *Atmos. Environ.* **2004**, *38*, 6467-6476.
39. Hering, S.; Fine, P.M.; Sioutas, C.; Jaques, P.A.; Ambs, J.L.; Hogrefe, O.; Demerjian, K.L. Field assessment of the Dynamics of Particulate Nitrate Vaporization Using Differential TEOM (R) and Automated Nitrate Monitors; *Atmos. Environ.* **2004**, *38*, 5183-5192.
40. Grover, B.D.; Kleinman, M.; Eatough, N.L.; Eatough, D.J.; Hopke, P.K.; Long, R.W.; Wilson, W.E.; Meyer, M.B.; Ambs, J.L. Measurement of total PM<sub>2.5</sub> Mass (Nonvolatile Plus Semivolatile) with the Filter Dynamic Measurement System Tapered Element Oscillating Microbalance Monitor; *J. Geophys. Res.* **2005**, *110*(D7), D07S03, doi:10.1029/2004JD004995.

#### About the Authors

Judith C. Chow and John G. Watson are Research Professors, and Douglas H. Lowenthal and Norman F. Robinson are Associate Research Professors, with the Desert Research Institute (DRI). Kihong Park was formerly an Assistant Research Professor at DRI and is currently an Assistant Professor at Gwangju Institute of Science and Technology. Karen A. Magliano is Chief of the Air Quality Data Branch at the California Air Resources Board. Address correspondence to: Judith C. Chow, Division of Atmospheric Sciences, Desert Research Institute, 2215 Raggio Parkway, Reno, NV 89512 ; phone: +1-775-674-7050; fax: 1-775-674-7009; e-mail: judyc@dri.edu.